



## 2D frequency domain finite-difference elastic-wave modeling

Alan A. V. B. Souza<sup>1</sup>, André Bulcão<sup>1</sup>, Bruno Pereira Dias<sup>1</sup>, Djalma M. Soares Filho<sup>1</sup>, Felipe de S. Duarte<sup>2</sup>, Felipe P. Loureiro<sup>3</sup>, \*Fernanda F. Farias<sup>1</sup>, Gustavo C. Alves<sup>1</sup>, Luiz A. Santos<sup>1</sup>, Ricardo F. C. C. da Cruz<sup>1</sup>;

<sup>1</sup> PETROBRAS, Brazil

<sup>2</sup> UFRJ/COPPE/LAMCE/LAB2M

<sup>3</sup> Fundação Gorceix

Copyright 2013, SBGf - Sociedade Brasileira de Geofísica

This paper was prepared for presentation during the 13<sup>th</sup> International Congress of the Brazilian Geophysical Society held in Rio de Janeiro, Brazil, August 26-29, 2013.

Contents of this paper were reviewed by the Technical Committee of the 13<sup>th</sup> International Congress of the Brazilian Geophysical Society and do not necessarily represent any position of the SBGf, its officers or members. Electronic reproduction or storage of any part of this paper for commercial purposes without the written consent of the Brazilian Geophysical Society is prohibited.

### Abstract

**We present a Finite Differences implementation of the 2D elastic wave equation. Our methodology makes use of both a staggered and a rotated grid, combining the stability and low phase dispersion of the two methods. The numerical simulation is done in the frequency domain, which allows us to easily implement an efficient boundary condition (PML) and enables the simulation of many sources simultaneously. We apply a compressed sparse matrix solver (LAPACK) and a vertical/horizontal displacement formulation in order to decrease the matrix demand for the implicit method. Results show the modeled snapshots in the time and frequency domains, which can be used as input for any seismic imaging process such as migration or Full Waveform Inversion.**

### Introduction

Seismic imaging is the main tool in exploration geophysics to model and interpret subsurface data. Nowadays, many techniques comprise our set of imaging tools, but some methods, such as Reverse Time Migration, Full Waveform Inversion and other wave propagation methods have gained importance due to their ability to handle complex geologies. Therefore, the ability to properly propagate seismic waves is crucial for the development and application of modern seismic tools.

However, traditional acoustic modeling may not be sufficient for a correct estimation of the forwardly propagated wavefield when the correct reflection amplitudes need to be predicted. Also, this type of modeling doesn't account for converted waves, which arise in compressional and shear waves for discontinuities in the medium and which have become more important with the widespread use of multicomponent data. In these cases, the full elastic wave equation must be solved.

Numerical solutions in the frequency domain can be advantageous when solving the elastic wave equation (Liao, 2009). However, care must be taken when implementing these solutions, mostly due to dispersion and computational costs. Amongst the many proposed methodologies for implementing finite difference modeling, we highlight the works by Stekl and Pratt (1998), Jo et al. (1996) and Liao et al. (2009).

Our approach to the problem of modeling the elastic equation was based on a combination of these different methods, taking advantage of their strengths in order to implement a reliable, computationally efficient (both in memory cost and processing time) algorithm that can be used for the computation of synthetic seismograms and as an input for inversion schemes, specially for Full Waveform Inversion.

### Methodology

The first step of our approach uses the viscoelastic wave equations in a heterogeneous 2D medium

$$\rho\omega^2 u + \frac{\partial}{\partial x} \left[ \lambda \left( \frac{\partial u}{\partial x} + \frac{\partial v}{\partial z} \right) + 2\mu \frac{\partial u}{\partial x} \right] + \frac{\partial}{\partial z} \left[ \mu \left( \frac{\partial v}{\partial x} + \frac{\partial u}{\partial z} \right) \right] = f \quad 1$$

and

$$\rho\omega^2 v + \frac{\partial}{\partial z} \left[ \lambda \left( \frac{\partial u}{\partial x} + \frac{\partial v}{\partial z} \right) + 2\mu \frac{\partial v}{\partial z} \right] + \frac{\partial}{\partial x} \left[ \mu \left( \frac{\partial v}{\partial x} + \frac{\partial u}{\partial z} \right) \right] = g \quad 2$$

Where  $\lambda$  and  $\mu$  are the Lamé parameters,  $u$  and  $v$  represent the horizontal and vertical components of the displacement vector,  $\rho$  stands for density,  $\omega$  corresponds to the angular frequency and  $f$  and  $g$  symbolize body forces.

Before discretizing equations (1) and (2), Stekl and Pratt (1998) extended the idea introduced by Jo et al. (1996) for the viscoacoustic case, where a 45 degree rotated coordinate frame is used in order to enhance the accuracy of the finite-difference approximation.

To obtain the equations in the rotated frame, we use their relationship with the standard coordinate system, which leads us to

$$\begin{aligned} \rho\omega^2 u + \frac{1}{2} \left\{ \frac{\partial}{\partial x'} \left[ (\lambda + 3\mu) \frac{\partial u}{\partial x'} \right] + \frac{\partial}{\partial z'} \left[ (\lambda + 3\mu) \frac{\partial u}{\partial z'} \right] \right. \\ \left. + \frac{\partial}{\partial x'} \left[ (\lambda + \mu) \frac{\partial v}{\partial x'} \right] - \frac{\partial}{\partial z'} \left[ (\lambda + \mu) \frac{\partial v}{\partial z'} \right] \right. \\ \left. - \frac{\partial}{\partial z'} \left[ (\lambda + \mu) \frac{\partial u}{\partial x'} \right] - \frac{\partial}{\partial x'} \left[ (\lambda + \mu) \frac{\partial u}{\partial z'} \right] \right. \\ \left. - \frac{\partial}{\partial z'} \left[ (\lambda - \mu) \frac{\partial v}{\partial x'} \right] + \frac{\partial}{\partial x'} \left[ (\lambda - \mu) \frac{\partial v}{\partial z'} \right] \right\} = f \end{aligned} \quad 3$$

and

$$\begin{aligned} \rho\omega^2 v + \frac{1}{2} \left\{ \frac{\partial}{\partial x'} \left[ (\lambda + 3\mu) \frac{\partial v}{\partial x'} \right] + \frac{\partial}{\partial z'} \left[ (\lambda + 3\mu) \frac{\partial v}{\partial z'} \right] \right. \\ \left. + \frac{\partial}{\partial x'} \left[ (\lambda + \mu) \frac{\partial u}{\partial x'} \right] - \frac{\partial}{\partial z'} \left[ (\lambda + \mu) \frac{\partial u}{\partial z'} \right] \right. \\ \left. + \frac{\partial}{\partial z'} \left[ (\lambda - \mu) \frac{\partial u}{\partial x'} \right] - \frac{\partial}{\partial x'} \left[ (\lambda - \mu) \frac{\partial u}{\partial z'} \right] \right. \\ \left. + \frac{\partial}{\partial z'} \left[ (\lambda + \mu) \frac{\partial v}{\partial x'} \right] + \frac{\partial}{\partial x'} \left[ (\lambda + \mu) \frac{\partial v}{\partial z'} \right] \right\} = g \end{aligned} \quad 4$$

With the aim of reducing numerical anisotropy, we write the viscoelastic equations as a linear combination of the two systems

$$\begin{cases} \rho\omega^2 u + aP_1 + (1-a)Q_1 = f \\ \rho\omega^2 v + aP_2 + (1-a)Q_2 = g \end{cases} \quad 5$$

Where  $P_1$  and  $P_2$  are the standard horizontal and vertical representation of the Laplacian operator, respectively, while  $Q_1$  and  $Q_2$  stand for the 45 degree rotated horizontal and vertical representations. The relative weight between standard and rotated grids is given by the coefficient  $a$ , which Jo et al. suggested to be searched in the region  $0 \leq a \leq 1$ .

At this point, it is possible to apply the second-order finite difference scheme for the partial derivatives found in Kelly et al. (1976). For the rotated frame, the necessary approximations can be found in Stekl and Pratt (1998).

Although we have already described one strategy to minimize the amount of numerical anisotropy, we set now another approach proposed by Jo et al. (1996) to reduce the overall numerical dispersion. To do that, we employ the lumped formulation, which uses the interpolation of the field values from the nearest node points and this interpolation is weighted by the density. Combining this with the consistent formulation, which approximates the density and fields to their values at each node, the approximation for homogeneous media becomes

$$\begin{aligned} \rho\omega^2 u_{m,n} \approx \rho\omega^2 b v_{m,n} + \rho\omega^2 \frac{(1-b)}{4} \\ \times (v_{m+1,n} + v_{m-1,n} + v_{m,n+1} + v_{m,n-1}) \end{aligned} \quad 6$$

for horizontal displacement. In equation 6, the coefficient  $b$  is chosen to minimize the numerical errors.

Before applying the discretization together with equations 5 and 6 in equations 4 and 3, we employed PML absorbing boundary conditions to attenuate the reflections whenever the wavefield reaches the model's boundaries. This process leads us to the finite-difference matrix equation:

$$A_i U_i = f_i \quad 7$$

Where  $U_i$  is a vector containing the displacement components,  $f_i$  is the source term and  $A_i$  is the coefficient matrix which is formed by  $2 \times 2$  matrixes.  $A_i$  is a massive sparse and banded matrix with dimensions of  $(2 \times n_x \times n_z) \times (2 \times n_x \times n_z)$ .

## Results

Verification of our modeling scheme was based on Liao et al. (2009), where a homogeneous model was used. The modeling parameters can be found in table 1.

Shear wave velocity	1333.3 m/s
Compressional wave velocity	2000 m/s
Density	2.073095 g/cm <sup>3</sup>
Time interval	0.001 s
Time samples	1024
Grid point interval	5 m
Model dimensions X and Z	200 x 200 grid points
Cutoff frequency	40 Hz

Table 1: Modeling parameters

For the PML boundary we add 40 grid points to each of the four sides of the model. Equation 7 is solved for several frequencies (1 – 41 Hz) and the inverse Fourier transform is applied in order to obtain the wavefield in the time domain.

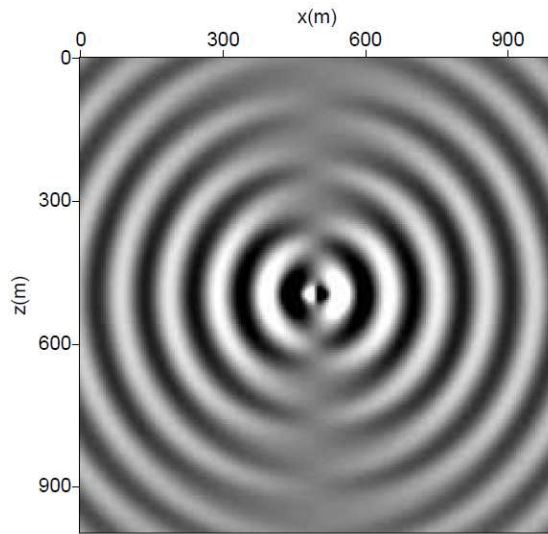


Figure 1: Snapshot of the horizontal displacement for 24 Hz.

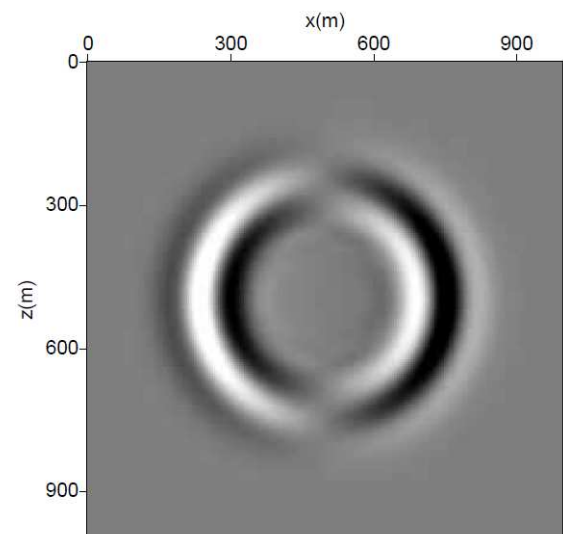


Figure 3: Snapshot of the horizontal displacement at 192 ms.

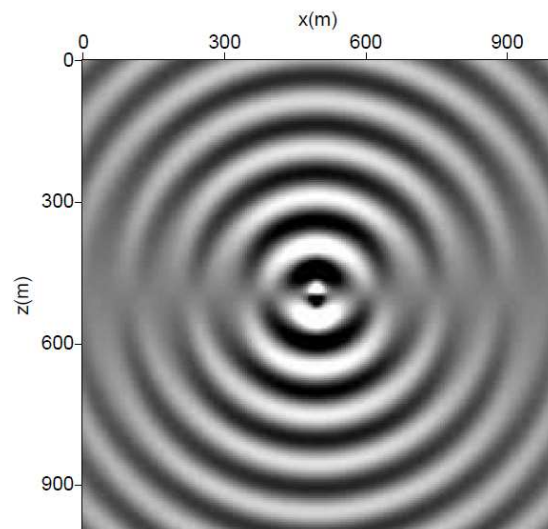


Figure 2: Snapshot of the vertical displacement for 24 Hz.

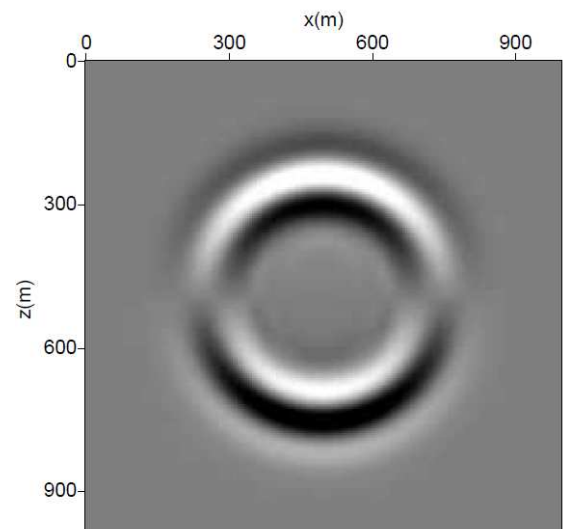


Figure 4: Snapshot of the vertical displacement at 192 ms.

## Conclusions

The modeling results obtained agree with those present in the literature, which demonstrates that the rotated grid and lumped formulation approaches can be combined into a single strategy to reduce dispersion and numerical anisotropy.

The matrix formulation based on the vertical and horizontal displacements significantly decreases the memory demands when compared to a velocity-stress formulation of the elastic wave equation, which would require the solution of a  $(5 \times n_x \times n_z) \times (5 \times n_x \times n_z)$ . This decrease is essential for any application of this modeling step in an inversion scheme, such as FWI.

## Acknowledgments

The authors would like to thank Petrobras for authorizing this publication.

## References

Stekl, I. and Pratt, R. G., 1998. Accurate visco-elastic modeling by frequency-domain finite differences using rotated operators: *Geophysics*, 63, 1779-1794.

Jo, C. H., Shin, C. S., and Suh, J. H., 1996. An optimal 9 point, finite difference, frequency-space, 2-d scalar wave extrapolator: *Geophysics*, 61, 529-537.

Liao, J., Wang, H. and Ma, Z 2009. 2-D frequency-space domain finite-difference elastic-wave modeling using compressed storage format.